

# Measurement of the $K_L$ nuclear interaction length in the NaI(Tl) calorimeter

---

**M. N. Achasov<sup>ab</sup>, K. I. Beloborodov<sup>ab\*</sup>, A. V. Berdyugin<sup>ab</sup>, A. G. Bogdanchikov<sup>a</sup>,  
A. V. Vasiljev<sup>ab</sup>, V. B. Golubev<sup>ab</sup>, T. V. Dimova<sup>ab</sup>, V. P. Druzhinin<sup>ab</sup>, A. A. Korol<sup>ab</sup>,  
S. V. Koshuba<sup>a</sup>, E. V. Pakhtusova<sup>a</sup>, S. I. Serednyakov<sup>ab</sup>, Z. K. Silagadze<sup>ab</sup> and  
Yu. V. Usov<sup>ab</sup>**

<sup>a</sup>*Budker Institute of Nuclear Physics, 630090 Novosibirsk, Russia*

<sup>b</sup>*Novosibirsk State University, 630090 Novosibirsk, Russia*

*E-mail: K.I.Beloborodov@inp.nsk.su*

**ABSTRACT:** In the study of the reaction  $e^+e^- \rightarrow K_S K_L$  at the VEPP-2M  $e^+e^-$  collider with the SND detector the nuclear interaction length of  $K_L$  meson in NaI(Tl) has been measured. Its value is found to be 30–50 cm in the  $K_L$  momentum range 0.11–0.48 GeV/c. The results are compared with the values used in the simulation programs GEANT4 and UNIMOD.

**KEYWORDS:** calorimeter,  $K$  meson nuclear interaction.

---

\*Corresponding author.

---

## Contents

<b>1. Introduction</b>	<b>1</b>
<b>2. Experiment</b>	<b>1</b>
<b>3. Selection of <math>e^+e^- \rightarrow K_S K_L</math> events</b>	<b>2</b>
<b>4. Extraction of the <math>K_L</math> nuclear interaction length</b>	<b>4</b>
<b>5. Conclusion</b>	<b>8</b>

---

## 1. Introduction

In the analysis of experimental data in the high-energy physics the Monte-Carlo (MC) simulation is widely used. There are known simulation packages, such as UNIMOD [1], GEANT3 [2], and GEANT4 [3], which successfully describe the physical processes of particles passage through the detector material. Nevertheless, in some cases, the accuracy of the theoretical models and/or the experimental data used in simulation may be not sufficient. Therefore, it is worthwhile to verify the simulation using new experimental data.

In  $e^+e^-$  annihilation into hadrons at the center-of-mass (c.m.) energies above 1 GeV the neutral kaons are intensively produced, e.g. in the process

$$e^+e^- \rightarrow K_S K_L. \quad (1.1)$$

Whereas  $K_S$  meson decays rapidly via  $K_S \rightarrow \pi\pi$  channel, the neutral  $K_L$  meson, due to its much greater lifetime, passes through detector material and is absorbed due to the nuclear interaction. Since kaons in the process (1.1) are producing in pairs, the  $K_L$  meson can be tagged by the recoiled  $K_S$  meson. This greatly facilitates the study of  $K_L$  interaction with the detector material.

In this paper we use kaons from the reaction (1.1) to measure the  $K_L$  nuclear interaction length in NaI(Tl) crystals in the momentum range from 0.11 to 0.48 GeV/c.

## 2. Experiment

The experiment on the study the  $e^+e^- \rightarrow K_S K_L$  process was carried out at the VEPP-2M [4]  $e^+e^-$  collider with the SND detector [5] in the c.m. energy range  $\sqrt{s} = 2E = 0.98\text{--}1.38$  GeV. The SND is a general purpose non-magnetic detector for low energy  $e^+e^-$ -colliders. In the center of the detector around the collider beam pipe a tracking system consisting of two drift chambers is installed. The main part of the SND is a three-layer spherical electromagnetic calorimeter based on 1640 NaI(Tl) crystals with the total weight 3.6 ton. The calorimeter covers the polar angle range

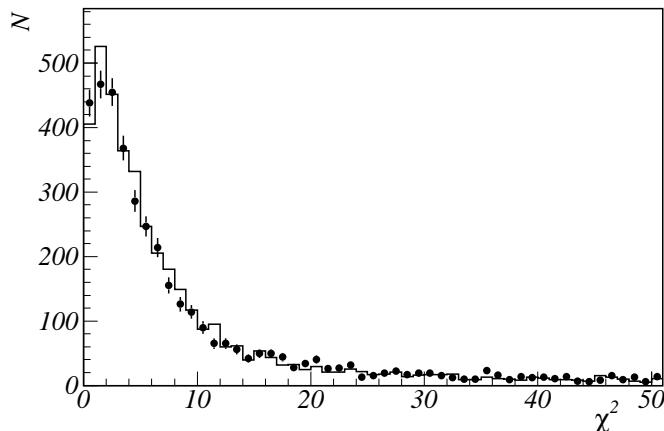


**Figure 1.** The distribution of  $\chi^2$  of the kinematic fit to the  $K_S \rightarrow \pi^0 \pi^0 \rightarrow 4\gamma$  hypothesis for  $K_S$  candidates in data (points with error bars) and  $e^+e^- \rightarrow K_S K_L(\gamma)$  simulation (histogram) at  $\sqrt{s} = 1.04 - 1.10$  GeV.

$18^\circ < \theta < 162^\circ$ . The crystal angular dimension is  $\Delta\theta = \Delta\phi = 9^\circ$ . The radial positions of the calorimeter layers are shown in Fig. 3. The total calorimeter thickness for particles originating from the interaction region is 34.7 cm ( $13.4X_0$ ), where  $X_0$  is the radiation length equal to 2.6 cm for NaI(Tl). Pairs of crystals of the two inner layers with thickness of 2.9 and  $4.8X_0$  are sealed in a common thin (0.1 mm) aluminum container. In the gap between the second and third calorimeter layers an aluminum supporting hemisphere is located. The scintillation light signals from the crystals are detected by vacuum phototriodes. Outside the calorimeter an iron absorber and a muon detector are placed.

In this paper the data collected in the energy interval  $\sqrt{s} = 1.04 - 1.38$  GeV with an integrated luminosity of  $9.2 \text{ pb}^{-1}$  are analyzed. These data were used previously to measure the  $e^+e^- \rightarrow K_S K_L$  cross section [6]. In addition, the data recorded at the maximum of the  $\phi(1020)$  resonance with an integrated luminosity of  $0.5 \text{ pb}^{-1}$  are used.

The Monte-Carlo event generator for the  $e^+e^- \rightarrow K_S K_L$  reaction used in this analysis includes radiative corrections [7]. In particular, an extra photon emitted by initial electrons is generated with the angular distribution modelled according to Ref. [8]. The  $e^+e^- \rightarrow K_S K_L$  Born cross section needed to calculate the radiative corrections is taken from Ref. [6].

The response of the SND detector is simulated using the UNIMOD package [1]. This package developed in BINP (Novosibirsk) in eighteens is functionally similar to the GEANT3 [2] simulation program. Special attention in UNIMOD is given to simulation of pion and kaon low-energy nuclear interactions. Nuclear cross sections are calculated with the SCATTER program [9], while the nuclear reactions are simulated using the NUCRIN model [10]. The simulation takes into account the variation of the detector and accelerator conditions (dead electronic channels, size of the interaction region, etc.) and beam-induced background photons and charged particles overlapping events of interest.

### 3. Selection of $e^+e^- \rightarrow K_S K_L$ events

The  $K_S$  mesons from the process  $e^+e^- \rightarrow K_S K_L$  decay inside the SND tracking system. The decay

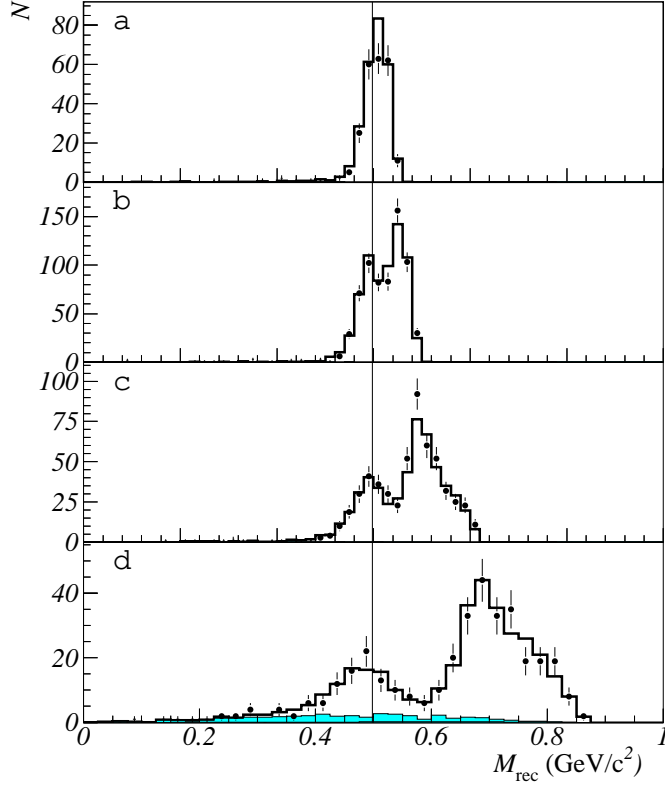


**Figure 2.** The  $M_{\text{rec}}$  spectrum for selected  $e^+e^- \rightarrow K_S K_L$  candidates in four energy intervals: (a)  $\sqrt{s} = 1.04 - 1.05$  GeV, (b)  $\sqrt{s} = 1.06 - 1.09$  GeV, (c)  $\sqrt{s} = 1.10 - 1.20$  GeV, and (d)  $\sqrt{s} = 1.20 - 1.38$  GeV. The shaded histogram shows the  $e^+e^- \rightarrow \omega\pi^0$  background. The vertical line indicates  $K_L$  mass.

mode  $K_S \rightarrow \pi^0\pi^0 \rightarrow 4\gamma$  is chosen for  $K_S$  reconstruction. Therefore we select events containing at least four photons and no charged particles. To eliminate the cosmic ray background, the veto from muon detector and the requirement that the fired calorimeter crystals do not lie along a straight line are used.

We combine four photons in an event to create a  $K_S$  candidate. Photons included into the  $K_S$  candidate must be in the polar angle range  $36^\circ < \theta_\gamma < 144^\circ$  and have the transverse energy profile in the calorimeter corresponding to the profile from single electromagnetic shower [11]. The four photons are kinematically fitted to the  $K_S \rightarrow \pi^0\pi^0 \rightarrow 4\gamma$  hypothesis. The distribution of  $\chi^2$  of the kinematic fit is shown in Fig. 1 for data and simulated  $e^+e^- \rightarrow K_S K_L$  events from the energy region  $\sqrt{s} = 1.04 - 1.10$  GeV, in which the background contribution is small. If more than one  $K_S$  candidate is found in an event, the candidate with the lowest  $\chi^2$  value is chosen. For further analysis, events with  $\chi^2 < 25$  are selected.

The dominant background process is  $e^+e^- \rightarrow \omega\pi^0 \rightarrow \pi^0\pi^0\gamma$ . To suppress this background the kinematic fit to the  $e^+e^- \rightarrow \pi^0\pi^0\gamma$  hypothesis is performed for events containing five or more photons. Events with  $\chi^2_{\pi^0\pi^0\gamma} < 60$  are rejected.

The measured  $K_S$  parameters are used to calculate the mass recoiling against the  $K_S$ :  $M_{\text{rec}} = \sqrt{(2E - E_{K_S})^2 - p_{K_S}^2}$ , where  $E_{K_S}$  and  $p_{K_S}$  are the  $K_S$  energy and momentum, respectively. The  $M_{\text{rec}}$  spectra for different energy intervals are shown in Fig. 2. The two peaks in the spectra for energies

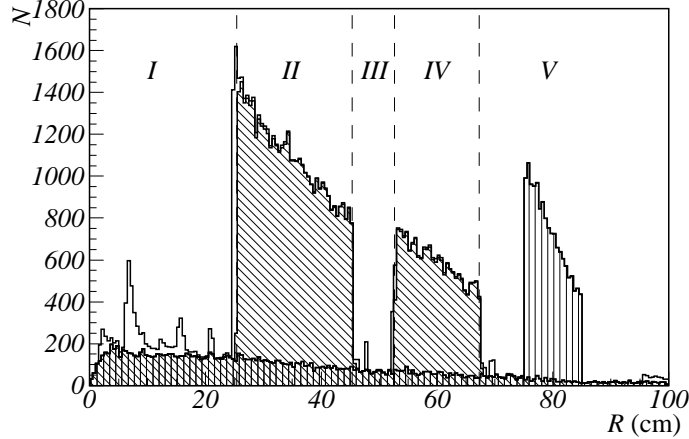


**Figure 3.** The simulated distribution of the radius of the disappearance point (due to decay or nuclear interaction) for  $K_L$  mesons with  $E = 0.51$  GeV. The cross-hatched histogram shows the contribution of  $K_L$  decays. The diagonally hatched areas in the zones II and IV show the contribution of nuclear interaction in NaI(Tl) crystals. The unhatched areas in the zones I, III and V represent the contribution of nuclear interaction in the detector material before the calorimeter, between the calorimeter layers, and after the calorimeter, respectively. The interaction in the iron absorber is shown by the histogram with vertical hatching. The deviation of the distribution for  $K_L$  decays from the exponential near zero is due to the finite size of the beam interaction region along the collider beam axis (radius is measured from the geometric center of the detector).

$\sqrt{s} > 1.06$  GeV correspond to the reactions  $e^+e^- \rightarrow K_S K_L$  and  $e^+e^- \rightarrow K_S K_L \gamma$ . The latter reaction is dominated by the radiative return to the  $\phi(1020)$  resonance, i.e. the process  $e^+e^- \rightarrow \phi \gamma$ . In the following analysis we use events with the recoil mass close to  $K_L$  mass ( $0.40 < M_{\text{rec}} < 0.55$  GeV/ $c^2$ ), which come from the  $e^+e^- \rightarrow K_S K_L$  reaction.

The distribution of selected events over energy intervals is given in Table 1. In the energy range above the  $\phi(1020)$  resonance ( $\sqrt{s} \geq 1.04$  GeV) 2606 events are selected. The background sources were studied in detailed in our earlier work [6]. The expected number of background events at  $\sqrt{s} \geq 1.04$  GeV is  $73 \pm 7$  (36 from the beam background, 25 from  $e^+e^- \rightarrow \eta \gamma$ , and 12 from  $e^+e^- \rightarrow \omega \pi^0$ ).

#### 4. Extraction of the $K_L$ nuclear interaction length

The  $K_L$  decay length  $\lambda_{\text{dec}}$  varies from 3.4 m at  $E = 0.51$  GeV to 15.2 m at  $E = 0.7$  GeV and far exceeds the calorimeter outer radius, about 0.7 m. The nuclear interaction length  $\lambda_{\text{int}}$  is close to the thickness of the calorimeter sensitive volume  $L_{\text{cal}} = 34.7$  cm. Therefore, a significant part of  $K_L$  mesons undergoes a nuclear interaction in the calorimeter. Charged particles and photons produced in the interaction give an energy deposition in NaI(Tl) crystals near the  $K_L$  path. Events selected using the criteria described above are divided into two classes, with four and with five or more photons. The latter class is dominated by events, in which the  $K_L$  mesons either decay or interact inside the detector volume.

Figure 3 shows the simulated radial distribution of the disappearance point (due to decay or nuclear interaction) for  $K_L$  mesons with  $E = 0.51$  GeV. It is seen that the main mechanism of the  $K_L$  disappearance inside the detector (zones I–IV in Fig. 3) is a nuclear interaction in NaI(Tl). From the experiment we extract the ratio of the number of events with five or more photons ( $N_{5\gamma} - N_{5\gamma,\text{bkg}}$ ) to the total number of events ( $N - N_{\text{bkg}} = N_{5\gamma} + N_{4\gamma} - N_{5\gamma,\text{bkg}} - N_{4\gamma,\text{bkg}}$ ), where  $N_{4\gamma}$  ( $N_{5\gamma}$ ) is the number of selected events with four (five or more) photons, and  $N_{4\gamma,\text{bkg}}$  ( $N_{5\gamma,\text{bkg}}$ ) is the estimated number of background events with four (five or more) photons.

The number of events with five or more photons can be calculated as follows:

$$\begin{aligned}
N_{5\gamma}^{\text{calc}} &= N_0 \sum_{i=1}^V r_i, \\
r_I &= w_I \varepsilon_I^{5\gamma}, \\
r_{II} &= w_{II} (1 - w_I) \varepsilon_{II}^{5\gamma}, \\
r_{III} &= w_{III} (1 - w_I) (1 - w_{II}) \varepsilon_{III}^{5\gamma}, \\
r_{IV} &= w_{IV} (1 - w_I) (1 - w_{II}) (1 - w_{III}) \varepsilon_{IV}^{5\gamma}, \\
r_V &= (1 - w_I) (1 - w_{II}) (1 - w_{III}) (1 - w_{IV}) \varepsilon_V^{5\gamma},
\end{aligned}$$

where  $N_0$  is the number of  $e^+e^- \rightarrow K_S K_L$  data events. The probabilities of the  $K_L$  disappearance in the NaI(Tl) (zones II and IV in Fig. 3) are equal to  $w_{II,IV} = 1 - \exp(-L_{II,IV}/\lambda)$ , where  $1/\lambda = 1/\lambda_{\text{int}} + 1/\lambda_{\text{dec}}$ ,  $L_{II}$  is the total thickness of the 1-st and 2-nd calorimeter layers, and  $L_{IV}$  is the thickness of the third layer. The  $\lambda_{\text{dec}}$  is calculated as an average over detected events from the energy interval under study.

The probabilities of  $K_L$  decay and nuclear interaction before the calorimeter  $w_I$  and between the calorimeter layers  $w_{III}$ , as well as the probabilities for an event to have five or more photons due to the disappearance in the  $i$ -th detector zone  $\varepsilon_i^{5\gamma}$  are obtained using MC simulation. The zone V in Fig. 3 contains  $K_L$  decays or interactions outside the calorimeter. Even in the absence of the  $K_L$  signal an event can be selected to the five-photon class, for example, because of the splitting electromagnetic shower of one of the photons from  $K_S$  decay.

The same formulae with the replacement of  $\varepsilon_i^{5\gamma}$  by  $\varepsilon_i^{4\gamma}$  are used to calculate the number of four-photon events. From the comparison of the predicted ratio  $N_{5\gamma}^{\text{calc}} / (N_{5\gamma}^{\text{calc}} + N_{4\gamma}^{\text{calc}})$  with the ratio obtained in data, the initial value of  $\lambda_{\text{int}}$  is obtained. The initial value is then corrected to take into account the following effects.

*$K_L$  elastic scattering.* The  $K_L$  elastic scattering leads to increase of the effective calorimeter thickness and approximately the same increase of the interaction length. The correction to  $\lambda_{\text{int}}$  varies from 7.4% at  $E = 0.51$  GeV up to 1.9% at  $E = 0.69$  GeV. The systematic uncertainty of this correction is estimated by variation of the elastic scattering cross section used in MC simulation by 30% and is found to be 2%.

*Beam-generated spurious photons.* About 10% of data events contain additional spurious photons from the beam background. The spurious photons lead to the transition of four-photon events to the five-photon class and decrease the measured  $\lambda_{\text{int}}$  value by about 10%. This effect is taken into account in MC simulation: the beam-background events recorded during experiment with a special random trigger are merged with simulated signal events. The  $e^+e^- \rightarrow \omega \rightarrow \pi^0 \gamma$  events are used to

**Table 1.** The energy interval ( $\sqrt{s}$ ), integrated luminosity ( $IL$ ), number of selected events ( $N$ ), number of background events ( $N_{\text{bkg}}$ ), number of events with five or more photons ( $N_{5\gamma}$ ,  $N_{5\gamma,\text{bkg}}$ ), and the measured  $K_L$  nuclear interaction length in NaI(Tl) ( $\lambda_{\text{int}}$ ). The first error in  $\lambda_{\text{int}}$  is statistical, the second systematic.

$\sqrt{s}$ , GeV	$IL$ , nb $^{-1}$	$N$	$N_{\text{bkg}}$	$N_{5\gamma}$	$N_{5\gamma,\text{bkg}}$	$\lambda_{\text{int}}$ , cm
1.02	486	30521	153	23840	127	$31.4 \pm 0.4 \pm 1.6$
1.04	70	245	3.0	183	2.1	$42.1 \pm 8.8 \pm 2.1$
1.05	264	556	7.2	433	5.9	$37.4 \pm 6.1 \pm 1.9$
1.06	432	656	6.6	514	4.7	$37.5 \pm 5.9 \pm 1.9$
1.07–1.08	669	516	8.9	391	5.1	$45.6 \pm 7.3 \pm 2.6$
1.09–1.10	531	206	5.8	156	4.2	$37.1 \pm 7.6 \pm 1.9$
1.11–1.13	508	118	6.9	82	4.4	$43.3 \pm 10.3 \pm 2.2$
1.14–1.16	674	101	5.9	73	4.1	$35.7 \pm 7.9 \pm 1.8$
1.18–1.21	1157	76	7.9	51	5.4	$48.3 \pm 13.8 \pm 2.4$
1.22–1.29	1916	83	9.8	55	6.7	$54.8 \pm 15.7 \pm 2.8$
1.30–1.38	2978	49	10.8	35	7.7	$45.7 \pm 21.6 \pm 2.4$

test that the simulation reproduces well the photon multiplicity distribution observed in data. The systematic uncertainty in the  $\lambda_{\text{int}}$  due to spurious photons is estimated to be less than 1%.

*Nonmonochromaticity of  $K_L$  mesons.* Radiative corrections, mainly due to the radiative return to the  $\phi$ -meson resonance, lead to the deviation of the  $K_L$  average energy from  $\sqrt{s}/2$ . This effect is especially significant in the range  $\sqrt{s} = 1.06 - 1.14$  GeV, in which the energies of  $K_L$  mesons from the reactions  $e^+e^- \rightarrow K_S K_L$  and  $e^+e^- \rightarrow \phi \gamma \rightarrow K_S K_L \gamma$  are already sizably different, while the peaks from these reactions in the  $M_{\text{rec}}$  spectra (Fig. 2b,c) are not well separated. The value of the nuclear interaction length measured in  $i^{\text{th}}$  energy interval ( $\lambda_i^{\text{meas}}$ ) is related to true  $\lambda_{\text{int},j}$  values for intervals with lower energies:

$$\lambda_i^{\text{meas}} = \sum_{j=1}^i P_{ij} \lambda_{\text{int},j}, \quad (4.1)$$

where  $P_{ij}$  is the probability for  $K_L$  produced at beam energy from  $i^{\text{th}}$  interval to have (due to initial state radiation) energy in  $j^{\text{th}}$  energy interval. The boundaries of the intervals listed in the first column of Table 1 are expanded to provide full coverage of possible  $K_L$  energies, e.g. the value of  $\lambda_{\text{int}}$  at  $\sqrt{s} = 1.06$  GeV are used in Eq.(4.1) for the range 1.055–1.065 GeV. The coefficients  $P_{ij}$  are determined from the  $K_L$  energy spectra obtained using MC simulation for different  $\sqrt{s}$ . The values of diagonal coefficients  $P_{ii}$  are about 0.5 for  $\sqrt{s} = 1.06 - 1.14$  GeV and then increase to about 0.9 at  $\sqrt{s} > 1.2$  GeV. The system of the linear equations (4.1) is solved to determine  $\lambda_{\text{int},j}$ . The systematic uncertainty in  $\lambda_{\text{int}}$  due to the  $K_L$  nonmonochromaticity is estimated to be 1% at  $\sqrt{s} = 1.02$  GeV, then increases reaching a maximum of 3% at  $\sqrt{s} = 1.08$  GeV, and then decreases to 1% at  $\sqrt{s} = 1.38$  GeV.

The procedure of  $\lambda_{\text{int}}$  measurement described above is tested using simulated  $e^+e^- \rightarrow K_S K_L(\gamma)$  events. The found nuclear interaction lengths are consistent with the values  $\lambda_{\text{int}}^{\text{MC}}$  used in simulation within the statistical uncertainties. The same result is obtained with  $\lambda_{\text{int}}^{\text{MC}}$  varied by 30%.

The corrected values of  $\lambda_{\text{int}}$  obtained in data are listed in Table 1. The first error is statistical, the second systematic. The sources of the systematic uncertainty are listed in Table 2. Some of them

**Table 2.** The sources of the systematic uncertainty on  $\lambda_{\text{int}}$  (%) for three  $K_L$  energies.

Source	0.52 GeV	0.54 GeV	0.69 GeV
$K_L$ elastic scattering	2.0	2.0	2.0
$K_L$ nonmonochromaticity	1.0	3.0	1.0
Spurious photons	1.0	1.0	1.0
$K_L$ interaction out of NaI(Tl)	3.4	3.4	3.4
Background subtraction	1.5	1.5	1.5
Detection efficiency	2.2	2.3	2.6
Total	5.0	5.8	5.2

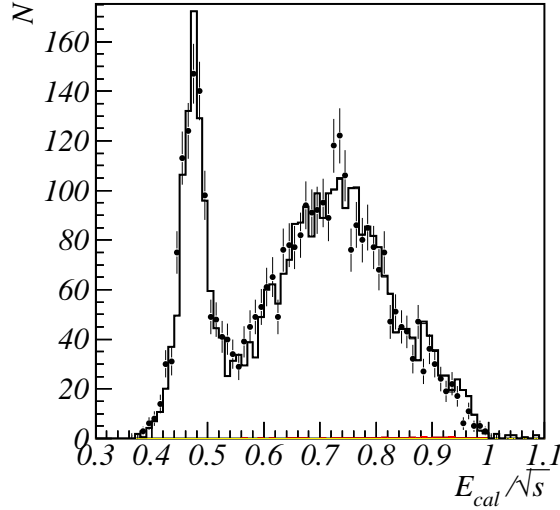


**Figure 4.** The distribution of the normalized energy deposition in the calorimeter for data events (points with error bars) and simulated  $e^+e^- \rightarrow K_S K_L(\gamma)$  events (histogram) at  $\sqrt{s} = 1.02$  GeV.

are described above. The uncertainty due to imperfect simulation of  $K_L$  nuclear interaction in the detector material before, after, and between the calorimeter layers is estimated by variation of the cross section used in the MC simulation by 30%. The uncertainty due to the background subtraction is determined by the uncertainties on the numbers of estimated background events in four- and five-photon classes. The systematic errors on the detection efficiencies,  $\epsilon_i^{5\gamma}$  and  $\epsilon_i^{4\gamma}$ , associated with  $K_S$  reconstruction are cancelled in the ratio  $N_{5\gamma}/(N_{5\gamma} + N_{4\gamma})$ . Remaining systematics is due to imperfect simulation of the detector response to  $K_L$  mesons. The distribution of the normalized energy deposition in the calorimeter  $E_{\text{cal}}/\sqrt{s}$  for selected data and simulated events at  $\sqrt{s} = 1.02$  GeV is shown Fig. 4. Good agreement between data and simulation spectra is seen. The narrow peak at  $E_{\text{cal}}/\sqrt{s} \approx 0.5$  corresponds to events with undetected  $K_L$  meson. Since the threshold on the  $K_L$  energy deposition is low (20 MeV), we do not expect any significant systematic uncertainty due to inaccuracy in the simulation of the detector response. The uncertainty in Table 2 associated with the detection efficiency is determined by simulation statistics.



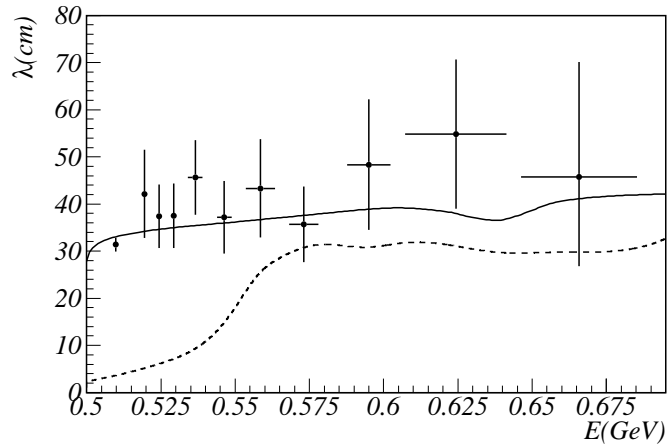


**Figure 5.** The  $K_L$  nuclear interaction length in NaI(Tl) as a function of the  $K_L$  energy. Points with error bars represent the result of this work. The solid curve shows the nuclear interaction length used in the UNIMOD [1] simulation package. The dotted line is the same dependence used in the GEANT4 package, version 9.5 (low-energy physics) [3].

## 5. Conclusion

Using kaons from the reaction  $e^+e^- \rightarrow K_S K_L$  we have measured the  $K_L$  nuclear interaction length in NaI(Tl) in the  $K_L$  energy (momentum) range from 0.51 (0.11) to 0.69 (0.48) GeV (GeV/c). The data were collected by the SND detector at the VEPP-2M  $e^+e^-$  collider. We did not find any other measurements of the  $K_L$  nuclear length at such low momenta in literature.

The energy dependence of the  $K_L$  nuclear interaction length measured in this work is shown in Fig. 5 in comparison with the nuclear lengths used in the UNIMOD [1] and GEANT4 [3] packages. The nuclear length for GEANT4 is obtained using test simulation, in which  $K_L$  mesons interact in a large block of NaI(Tl). The  $\lambda_{\text{int}}^{\text{MC}}$  is calculated from the probability of  $K_L$  disappearance in a thin layer of material.

Our data are in good agreement with UNIMOD. The values of the nuclear length used in GEANT4 version 9.5 (the model of hadron physics FTFP\_BERT [12]) contradict to the measured values at energies below 0.55 GeV. The results of this work may be used to refine the  $K_L$  nuclear cross section in GEANT4.

## Acknowledgments

This work is supported by Russian Science Foundation (project No. 14-50-00080).

## References

- [1] A. D. Bukin *et al.*, Preprint INP 86-18, Novosibirsk, 1986.
- [2] R. Brun, F. Bruyant, M. Maire, A. C. McPherson and P. Zanmarini, CERN Report No. CERN-DD/EE/84-1, 1987.
- [3] S. Agostinelli *et al.*, Nucl. Instrum. Methods Phys. Res., Sect. A **506**, 250 (2003); J. Allison *et al.*, IEEE Trans. on Nucl. Science **53**, 270 (2006).

- [4] A. N. Skrinsky, “VEPP-2M status and prospects, and  $\phi$ -factory project at Novosibirsk,” in Proc. of Workshop on physics and detectors for DAΦNE 95, 1995, vol.IV, p.3.
- [5] M. N. Achasov *et al.*, Nucl. Instrum. Methods Phys. Res., Sect. **A449**, 125 (2000).
- [6] M. N. Achasov *et al.*, JETP **103**, 720 (2006).
- [7] E. A. Kuraev and V. S. Fadin, Sov. J. Nucl. Phys. **41**, 466 (1985) [Yad. Fiz. **41**, 733 (1985)].
- [8] G. Bonneau and F. Martin, Nucl. Phys. B **27**, 381 (1971).
- [9] A. M. Makhov, Preprint INP 92-66, Novosibirsk, 1992.
- [10] K. Haenssger *et al.*, Preprint KMU-HEP, 80-07, Leipzig, 1980.
- [11] A. V. Bozhenok, V. N. Ivanchenko and Z. K. Silagadze, Nucl. Instrum. Methods Phys. Res., Sect. **A379**, 507 (1996).
- [12] Geant4 Physics Reference Manual, in <http://cern.ch/geant4/support/userdocuments.shtml> [cern.ch]